ACTA NEUROBIOLOGIAE EXPERIMENTALIS

Acta Neurobiol Exp 2006, 66: 43-54

Stereotactic approach and electrophysiological characterization of thalamic reticular and dorsolateral nuclei of the juvenile pig

Martin Gerbert Frasch[1,2], Bernd Walter[3], Michael Brodhun[4], Holger Friedrich[1], Michael Eiselt[1], and Reinhard Bauer[1]

[1]Institute for Molecular Cell Biology, Pathophysiology Laboratory, [2]Department of Neurology, [3]Department of Neurosurgery, [4]Institute of Pathology, Universitätsklinikum Jena, Friedrich Schiller University, D-07740 Jena, Germany

Abstract. Few reports exist on complex functions of pig's central nervous system. A direct access to thalamic structures enables a deeper understanding of neuronal networks. Here we present an easy to implement stereotactic approach to reach both reticular and dorsolateral thalamic nuclei (RTN and LD). In thirteen pigs (7 weeks old) the correct electrode position was confirmed for 22 out of 26 thalamic electrodes (RTN: A+2, L9, V24 and LD: A-2, L5, V20, with bregma A 0, L 0). Quantitative effects of isoflurane/nitrous oxide (State 1) and fentanyl sedation (State 2) were determined by brain hemodynamics and metabolism. Neurophysiologic features were performed by spectral power, coherence and SEP analysis. Brain blood flow (by 21 ± 13%) and oxidative brain metabolism ($CMRO_2$ by 26 ± 12%, $CMR_{Glucose}$ by 26 ± 22%) were markedly reduced during State 1 ($P<0.05$). Regional thalamic blood flow exhibited similar alterations, but side-differences did not occur. State 1 induced quite similar brain activity in cortical as well as thalamic regions investigated. During State 2 electrocortical activity of low frequency ranges was markedly reduced, whereas spectral band power of high frequency ranges was additionally decreased in RTN ($P<0.05$). Thus, we used a convenient approach for targeted deep electrode implementation and characterized electrophysiological features in RTN and LD.

The correspondence should be addressed to R. Bauer, Email: Reinhard.Bauer@mti.uni-jena.de

Key words: reticular thalamic nucleus, dorsolateral thalamic nucleus, stereotaxy, sedation, isoflurane, fentanyl, electrophysiology, swine

INTRODUCTION

The domestic pig is increasingly used in neuroscience for methodological approaches (Andrews et al. 1990, Mount and Ingram 1971, Okada et al. 1999, Zwiener et al. 1983) and applied neurophysiological research including traumatic and hypoxic-ischemic brain injury (Bauer et al. 1999, Fritz et al. 1999, Goel et al. 1996, Kirsch et al. 1990, Sherman et al. 1999, Walter et al. 2000), brain development (Jarvinen et al. 1998), biocompatibility of neural implants (Williams et al. 1999) and depth of sedation (Martoft et al. 2001). Beside relatively low costs and easy availability the main reason for using this species to create clinic-like animal models of acute and/or chronic brain disorders results both from the anatomical and physiological resemblances to those of humans. Amongst others it is relatively large and gyrencephalic, which facilitates its usage as pathogenetic or experimental therapeutic models such as surgical intervention, traumatic brain injury, installation of electrodes and the placement of injections (Fritz et al. 2005).

Until now, reports on complex functions of pig's central nervous system remained rare. However, decisive integrative functions can only be analyzed if a simultaneous estimation of brain activity of key structures of the desired neuronal network can be obtained. A direct access to thalamic structures would enable a deeper understanding of underlying neurophysiological processes of a key interface between peripheral, brain stem and forebrain structures. This applies especially to such an intriguing area as reticular thalamic nucleus (RTN) implied in various complex cerebral activities like different states of vigilance including sleep and sedation as well as changes during and after brain injury (Alkire et al. 2000, Fiset et al. 1999, Pace-Schott and Hobson 2002, Ross et al. 1993, Steriade 2001). Further key structures of such a functional network represent the thalamic relay nuclei for specific information, like dorsolateral thalamic nucleus (LD) and forebrain target regions, like somatosensory cortex (Jones 1985).

To study neurophysiological features of thalamic entities in the pig, a target-oriented stereotactic approach including suitable stereotactic apparatus and coordinates are essential. Whereas several stereotactic instruments have been developed for pig skull and brain (Dellmann and McClure 1966, Marcilloux et al. 1989, Poceta et al. 1981, Salinas-Zeballos et al. 1986), any reports with detailed description of successful sensor implantation and related stereotactic coordinates for thalamic regions of interest are lacking.

Aim of the present study was to determine stereotactic coordinates of the reticular thalamic and dorsolateral nuclei in juvenile pigs using a commonly available stereotactic apparatus with an experimental approach based on external skull structures such as bregma and sagittal suture. Furthermore, spontaneous and evoked field potential activity of RTN, LD and corresponding electrocorticographic activity (ECoG) were quantitatively characterized under different sedation states. We used a substantial experimental approach including quantification of regional CBF and brain oxidative metabolism to verify reproducible experimental conditions.

METHODS

Experiments were carried out in accordance with the European Communities Council Directive 86/609/EEC for animal care and use. Laboratory animal protocols were approved by animal research committee of the Thuringian State government.

General instrumentation

Thirteen female juvenile pigs of mixed German domestic breed (7 weeks old, weighing 15.1 ± 1.3 kg) were sedated with intramuscular injection of ketamine hydrochloride (20 mg/kg b.w.), midazolam (1 mg/kg b.w.). Thereafter animals were initially anesthetized with 2.5% isoflurane (inspired concentration) in nitrous oxide and oxygen (FiO_2 = 0.35–0.40) delivered by a mask. The anesthesia was maintained throughout the surgical procedure with an inspired concentration of 1.5% isoflurane. Additionally, incision sites were infiltrated with 1% lidocaine. Tracheotomy (tube size: 5.5 mm I.D.) was performed and a central venous catheter was advanced *via* left external jugular vein to the upper caval vein for drug administration and fluid therapy (physiologic saline: 5 mL/kg b.w./h). Muscle relaxation was achieved with pancuronium bromide (0.2 mg/kg b.w./h, i.v.). All animals were ventilated in a pressure controlled mode (Servo Ventilator 900C, Siemens-Elema, Sweden). Ventilation was controlled by continuous endexpiratory CO_2 monitoring and hourly arterial blood gas check. The ventilator was set with a positive inspiratory pressure of 15 to 20 mbar

and a positive end-expiratory pressure of 2 to 4 mbar. Respiratory rate and inspired oxygen fraction were titrated to maintain normoxic and normocapnic conditions.

Body temperature was controlled by a rectal thermoprobe, maintained throughout instrumentation at 37.5 ± 0.5°C using a water-filled pad connected to a heating-cooling thermostat and a feedback controlled heating lamp. The urinary bladder was punctured and permanently drained (Cystofix, Braun Melsungen AG, Germany). Both saphenous arteries were catheterized and were advanced into the abdominal aorta and positioned 1 cm above the aortic bifurcation for continuous arterial blood pressure monitoring and in order to withdraw reference samples for the colored microsphere measurements (see below). In addition a left thoracotomy was then performed through the third intercostal space and a catheter was inserted into the left atrium for injection of colored microspheres for multiple regional cerebral blood flow measurements (Walter et al. 1997). Arterial and central venous catheters were connected with pressure transducers (P23Db, Statham Instruments, Puerto Rico). An electrocardiogram was recorded from standard limb leads using stainless steel needle electrodes. Correct positions of the catheter tips were checked by continuous pressure trace recordings and by autopsy at the end of the experiment.

Instrumentation of the head

The animal was placed in sphinx position with the head fixed in a stereotactic frame (Kopf Instruments, Tujunga, CA, USA). The head was fixed by ear bars placed in the auditory canals, mouth bars and nose pieces. Thereafter head and apparatus fitted tightly together and the interaural axis was made horizontal with the help of an air spirit level. Horizontal plane was then determined by appropriate adjustment of the aural lower orbital ridge line. After exposing the skull trepanations were made for stereotactic placement of ten electrocorticographic electrodes for bihemispherial leads from frontal, parietal, central, temporal and occipital regions (Fig. 1) and guides for insertion of electrodes into the left thalamus (centrodorsal part of reticular nucleus (RTN, 2 mm anterior to bregma, 9 mm lateral to bregma, 24 mm ventral to dura) and the dorsolateral thalamic nucleus (LD, 2 mm posterior to bregma, 5 mm lateral to bregma, 20 mm ventral to dura). The stereotactic coordinates of thalamic electrodes (RTN and LD) were predetermined in three pigs of the same age based on own experiences (Kuhnen et al. 1999) and appropiate reference (Félix et al. 1999). Using a micromanipulator (Kopf Instruments, Tujunga, CA, USA) guides for thalamic electrodes were inserted (∅ 0.9 mm), followed by insertion of the insulated unipolar silver/silver chloride electrodes. The length of the recording tip of the depth electrodes amounted to 2 mm. An additional polyurethane catheter (inner diameter 0.3 mm) was inserted into the superior sagittal sinus through a midline burr hole (3 mm in diameter and located 4 mm caudal to the bregma) and advanced to the confluence of the sinuses to obtain brain venous blood samples (Fig. 1). All trepanation sites were closed with bone wax and dental acrylic. Correct electrode placement was confirmed by necropsy and histological evaluation (Fig. 1). For SEP acquisition two electrodes were fixed epidermally on the left and right side of pig's snout corresponding to the area of maxillar nerve.

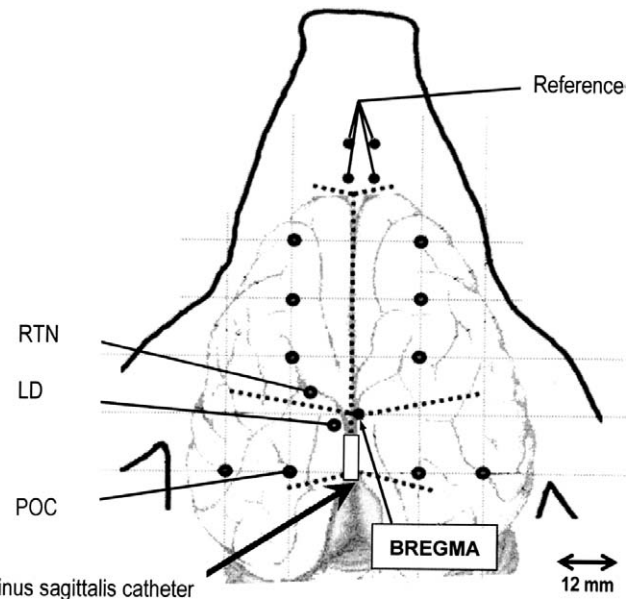

Fig. 1. Schematic representation of electrode localizations. Dotted lines mark cranial sutures; (POC) derivation from parieto-occipital cortex; (RTN) derivation from centrodorsal part of reticular nucleus; (LD) derivation from dorsolateral thalamic nucleus. For further details see text.

Experimental protocol

After the surgical preparation had been completed, the anesthesia was set to an inspired concentration of

1.3 % isoflurane in 70% nitrous oxide and 30% oxygen and the piglets were allowed to stabilize for 90 minutes. Subsequently, series of spontaneous and somatosensory evoked brain activity were recorded at two different states of sedation [isoflurane/nitrous oxide anesthesia (State 1), fentanyl analgesia (State 2)]. This was followed by CBF measurement and blood sample withdrawal. First during State 1 series of measurements were performed. Then, isoflurane and nitrous oxide were removed from inspired gas. Ventilation with 100% O_2 was preceded for 5 minutes and continued by an air/O_2 mixture. After i.v. bolus injection of fentanyl (0.3 mg) a continuous iv infusion of fentanyl (0.015 mg/kg body weight/h) was performed. A second series of measurements (State 2) was done so that CBF measurement occurred 60.7 ± 6.1 min after isoflurane/nitrous oxide removal.

At the end of the experiment, animals were prepared for perfusion fixation of the brain. Bilateral insertions of polyethylene catheters (inner diameter 1.8 mm) were performed into both common carotid arteries in rostral direction and secured. Subsequently, 30% potassium chloride solution was injected intracardially, so that heart beat stopped immediately. The head was immediately perfused by warmed saline, and when the disconnected central venous catheter outflow was mainly blood-free perfusion was continued with 5% buffered formaldehyde. Thereafter, head was removed and placed into buffered formaldehyde solution (5%, pH 7.4) for 7 days for further in situ fixation. The brain was then removed and electrode positions were determined histologically by preparation of serial coronal slices. Coordinates were estimated according to Felix and coauthors (1999).

Data acquisition and analysis

The regional CBF was measured by means of the reference sample color-labeled microsphere (DyeTrak®, Triton Technology, San Diego, CA, U.S.A.) technique, which represents a valid alternative to the radioactively labeled microsphere method for organ blood flow measurement in pigs and avoids all disadvantages arising from radioactive labeling with long-lived isotopes (Walter et al. 1997). Application in piglets and methodical considerations are presented and discussed in detail elsewhere (Bauer et al. 1996, Walter et al. 1997). Briefly, in random sequence about three million colored polystyrene microspheres were injected into the left atrium. A blood sample was withdrawn from the thoracic aorta as the reference sample. The injection line was then flushed with 2-ml saline. A blood sample was withdrawn from the abdominal aorta as the reference sample, beginning 15 seconds before the microsphere injection and continuing for 2 minutes at a rate of 3.53 ml/min (syringe pump SP210iw, World Precision Instruments Inc., Sarasota, Fl, U.S.A.). At the end of each experiment, the brains were removed and sectioned in the desired brain regions. For digestion, reference blood samples and tissue samples between 0.5 and 2.5 g were covered with an appropriate volume (approximately 3 ml/g) of digestive solution (4 N KOH with 4% Tween 80 in deionized water). All tissue and blood samples were digested for a minimum of 4 h at 60°C. In order to isolate the microspheres, each digested tissue sample was then filtered under vacuum suction through an 8-µm pore polyester-membrane filter. Colored microspheres were quantified by their dye content. The dye was recovered from the microspheres by adding dimethylformamide. The photometric absorption of each dye solution was measured by a diode array UV/visible spectrophotometer (Model 7500, Beckman Instruments, Fullerton, CA, U.S.A.). Calculations were performed using the MISS® software (Triton Technology, San Diego, CA, U.S.A.). The number of microspheres was calculated using the specific absorbance value of the different dyes. All reference and tissue samples contained > 400 microspheres.

Heart rate, mean arterial blood pressure (MABP), arterial and brain venous pH, PCO_2, and PO_2, oxygen saturation, glucose, lactate and hemoglobin values were measured immediately before the microsphere injection, respectively. Blood pH, PCO_2, and PO_2 were measured with a blood gas analyzer (model ABL50, Radiometer, Copenhagen, Denmark), blood hemoglobin and oxygen content were measured using a hemoximeter (model OSM3, Radiometer, Copenhagen, Denmark), and blood glucose and lactate contents were measured with an electrolyte, metabolite laboratory EML105® (Radiometer, Copenhagen, Denmark) and corrected to the body temperature of the animal at the time of sampling.

The absolute flows to the tissues measured by the colored microspheres were calculated by the formula:

$flow_{tissue}$ = number of $microspheres_{tissue}$ × ($flow_{reference}$ / number of $microspheres_{reference}$). Flows are expressed in milliliters per min per 100g tissue by normalizing for tissue weight. The $CMRO_2$ and $CMR_{Glucose}$ were obtained by multiplying the blood flow to the forebrain by the cerebral arteriovenous O_2 as well as glucose content difference, respectively. The blood flow to the forebrain includes all regions drained by the sagittal sinus (cerebral cortex, cerebral white matter, some deep gray structures: basal ganglia, thalamus, and hippocampus) (Coyle et al. 1993).

Unipolar electrocortico- and electrothalamogramm (ECoG, EThG) were amplified, filtered (time constant was 0.1 seconds, cut off frequency was 1000 Hz), fed into a PC using a 16 channel A/D board (Data Translation, DT2821F, Marlboro, MA) and stored together with arterial blood pressure and body temperature on a hard disk for off-line data analysis (sample rate was 125 Hz). All ECoG and EThG channels were visually controlled for any artifacts. We found no disturbances in ECoG and EThG through EKG and respiration signals. The animals were well treated with muscle relaxants, so no artifacts through activity of striated muscles or body movements were found (Rampil et al. 1988). Using data acquisition software (Watisa®, GJB Datentechnik Bolten & Jannek GbR, Ilmenau) and an own Matlab-based analysis software (Matlab® 6.1, R13) 300 sec ECoG and EThG intervals consisting of 10 consecutive intervals per 30 s at each experimental period were selected and regional electrical brain activity was quantified using Fast Fourier Transformation (FFT) by averaged power and cross-power spectra and expressed as the grand mean of the power spectral density and coherence (delta band: 1.5–4 Hz, theta band: 4–8 Hz, alpha band: 8–13 Hz, beta band: 13–20 Hz, gamma band: 20–40, whole frequency band: 1.5–40 Hz).

Somatosensory evoked potentials (SEPs) were induced by bipolar application of constant current rectangular impulses (70 μs, 5 mA applied at 1 pulse/s (HES-Stimulator T, Fa. Hugo Sachs Elektronik, Hugstetten, Germany), for 2 minutes at every side, respectively, sampled with 2 kHz and averaged the data across 100 sweeps. Latencies were first detected visually in each animal between 12 and 80 ms corresponding to the time frame of middle latency SEP (Niedermeyer and Da Silva 1999) expected under sedation and interindividually reproducible latencies were selected. Subsequently, for each determined latency the corresponding amplitude was estimated as the perpendicular projected distances between trough and peak components of the respective EP trace (Martoft et al. 2001) and presented as grand means together with amplitude and latency distribution of significant EP deviations.

Table I

Effect of different sedation states (State 1 – isoflurane/nitrous oxide anesthesia; State 2 – fentanyl analgesia) on systemic and cerebral hemodynamic and metabolic parameters, arterial blood gases and acid-base balance in juvenile piglets

	State 1	State 2
mean arterial blood pressure (mm Hg)	67 ± 8	100 ± 13*
heart rate (min^{-1})	180 ± 44	225 ± 40*
arterial pCO_2 (mm Hg)	36 ± 3	39 ± 3*
arterial pH	7.50 ± 0.03	7.45 ± 0.05*
arterial base excess (mmol × L^{-1})	4.9 ± 1.8	3.2 ± 2.6*
arterial pO_2 (mm Hg)	121 ± 18	146 ± 29
arterial glucose (mmol × L^{-1})	6.1 ± 1.5	7.1 ± 2.4*
arterial lactate (mmol × L^{-1})	1.8 ± 0.7	2.4 ± 1.7*
CBF (ml × h × $100g^{-1}$ × min^{-1})	46 ± 10	58 ± 11*
$CMRO_2$ (ml × h × $100g^{-1}$× min^{-1})	2.6 ± 0.7	3.4 ± 1.0*
$CMR_{Glucose}$ (μm × h × $100g^{-1}$× min^{-1})	30 ± 8	44 ± 14*

Values are presented as means ± SD; n=12; (*) P<0.05. (*) Significant differences between State 1 and State 2; (CBF) cerebral blood flow; ($CMRO_2$) cerebral oxygen consumption; ($CMR_{Glucose}$) cerebral glucose consumption.

Statistical analysis

If not otherwise indicated, data are reported as mean ± SD. Comparisons between the different sedation states were made with paired *t*-tests. Differences were considered significant when $P<0.05$. Physiological data have been obtained from twelve animals. One swine must be excluded because of progressive hyperthermia development during isoflurane anesthesia.

RESULTS

Physiological data are presented in Table I. Blood gas values, acid-base balance and parameters of systemic metabolism were within physiological ranges under both sedation states investigated. However, MABP (by 32 ± 11%) and heart rate (by 24 ± 15%) as well as CBF (by 21 ± 13%) and oxidative brain metabolism ($CMRO_2$ by 26 ± 12%, $CMR_{Glucose}$ by 26 ± 22%) were markedly reduced during State 1 ($P<0.05$), compared with State 2. Regional thalamic blood flow exhibited similar alterations under the two different states of sedation. However, side-differences did not occur (Fig. 2).

Regional electrophysiological activity was visually assessed and quantified by power spectral analysis and quantitative SEP analysis. State 1 induced quite similar brain activity in cortical as well as thalamic regions investigated, with predominant spectral power in the low frequency delta and theta bands representing 79 ± 11% to 87 ± 11% of total spectral power (Fig. 3). In addition, during State 1 a prominent peak in power spectra around 20 Hz was observed in the cortical and thalamic derivations (Fig. 4).

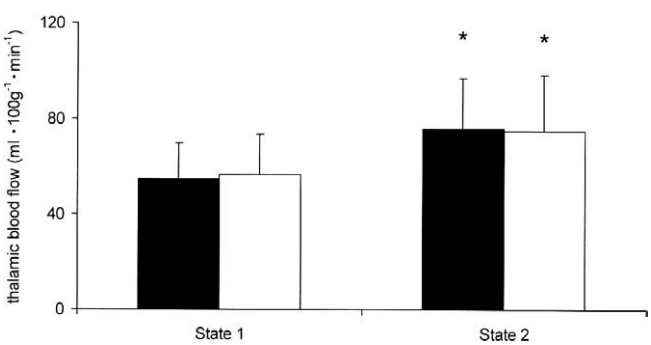

Fig. 2. Bilateral thalamic blood flow (black columns – left side containing deep electrode implantations; open columns – right side) of juvenile piglets (n=12; *$P<0.05$, significant differences between isoflurane/nitrous oxide anesthesia (State 1) and fentanyl analgesia (State 2)).

During State 2 electrical regional brain activity over POC was markedly reduced to 38–51% compared to State 1, mainly induced by diminished activity of low frequency ranges, whereas in RTN the spectral band power in high frequency ranges also decreased (Fig. 4,

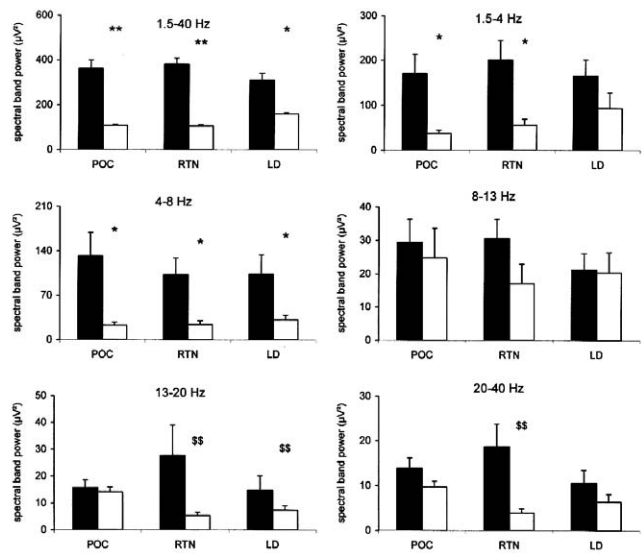

Fig. 3. Effect of different sedation states (black columns – isoflurane/nitrous oxide anesthesia (State 1); open columns – fentanyl analgesia (State 2)) on spectral band power of cortical (parieto-occipital region, POC) and thalamic (centrodorsal part of reticular nucleus (RTN), dorsolateral thalamic nucleus (LD)) brain activity of juvenile piglets (n=8). Mean ± SEM, (*$) $P<0.05$; (**$$) $P<0.01$. (*) Significant differences between State 1 and State 2; ($) significant differences compared with POC).

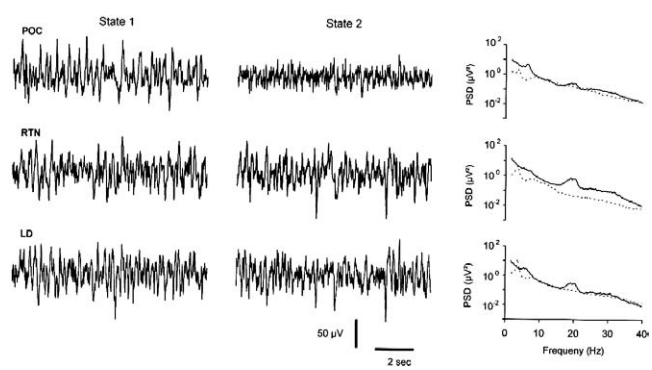

Fig. 4. Representative recordings (left panel) and grand mean of power spectral density (PSD, right panel), derived from 10 consecutive periods of 30 s duration of regional brain activity from juvenile pigs (n=8) during isoflurane/nitrous oxide anesthesia (State 1, full lines in PSD plots) and fentanyl analgesia (State 2, dotted lines in PSD plots).

Table II

Effect of different sedation states (State 1 – isoflurane / nitrous oxide anesthesia; State 2 – fentanyl analgesia) on spectral coherence in juvenile piglets

		State 1	State 2
Coherence	Frequency bands		
POC-RTN	whole band	0.80 ± 0.10*	0.69 ± 0.07§
	delta band	0.59 ± 0.08	0.57 ± 0.04
	theta band	0.63 ± 0.03	0.65 ± 0.09
	alpha band	0.62 ± 0.05*	0.50 ± 0.15§
	beta band	0.65 ± 0.27*	0.39 ± 0.22§
	gamma band	0.36 ± 0.36*	0.00 ± 0.00
POC-LD	whole band	0.76 ± 0.19$	0.77 ± 0.07$
	delta band	0.56 ± 0.09$	0.61 ± 0.09$
	theta band	0.58 ± 0.23$	0.72 ± 0.11$
	alpha band	0.53 ± 0.22$	0.58 ± 0.09$
	beta band	0.52 ± 0.35$	0.52 ± 0.21
	gamma band	0.23 ± 0.32	0.05 ± 0.15
RTN-LD	whole band	0.89 ± 0.10	0.90 ± 0.05#
	delta band	0.80 ± 0.12#	0.88 ± 0.05#
	theta band	0.77 ± 0.27	0.88 ± 0.06#
	alpha band	0.73 ± 0.30	0.71 ± 0.17#
	beta band	0.63 ± 0.41	0.57 ± 0.33#
	gamma band	0.26 ± 0.34	0.04 ± 0.11

Values are presented as mean ± SD; n=8; (*), (§), (#), ($) P<0.05. (*) Significant differences between State 1 and State 2; (§), (#), ($) differences in coherence between POC-RTN vs. POC-LD, POC-RTN vs. RTN-LD and POC-LD vs. RTN-LD, respectively. (POC) parieto-occipital cortex; (RTN) reticular thalamic nucleus; (LD) dorsolateral thalamic nucleus.

P<0.05, P<0.01). In LD, the spectral band power decreased during State 2 in the whole and theta band, only (P<0.05). Furthermore, relative distribution of spectral band power remained sustained in thalamic activities, whereas the proportion of higher frequency band power was markedly increased in the cortical brain activity representing 45 ± 8% of total spectral power, compared to 17 ± 4% at State 1 (P<0.01).

In State 2, POC-RTN coherences in whole, alpha and beta frequency bands were lower than POC-LD coherences (Table II, P<0.05). In State 1, such differences were not detected. In both states RTN-LD coherence was higher than POC-RTN coherence in all but beta frequency band (P<0.05). In this band POC-RTN coherence was higher than RTN-LD coherence in state 1, but not in state 2 (P<0.05). In State 1, RTN-LD coherence was higher than POC-LD coherence in delta frequency band, whereas in State 2 this occurred in all frequency bands (P<0.05). Coherence between POC and RTN was increased in State 1 in the whole frequency band as well as in alpha and beta frequency bands (Table II, P<0.05). It disappeared completely in State 2 in gamma band. This was also true for POC-LD and RTN-LD coherences. The latter did not change significantly in other frequency bands. SEP was most pronounced in the cortical derivation (Fig. 5, P<0.05).

Histological evaluation revealed that 22 out of 26 thalamic electrodes were correctly implanted (Fig. 6). In one case both electrodes were about 2 mm outside the target region. In two further animals the electrode tips of either LD or RTN electrodes were outside the target region.

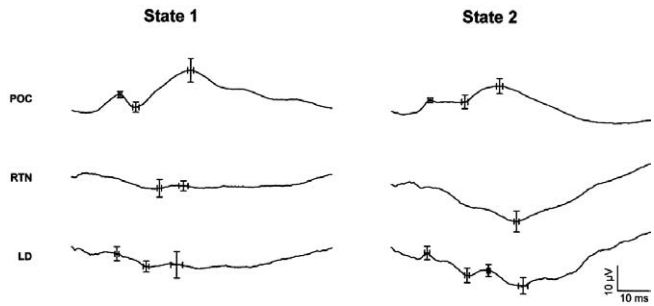

Fig. 5. Effect of different sedation states (isoflurane/nitrous oxide anesthesia (State 1); fentanyl analgesia (State 2)) on middle latency SEP of cortical (parieto-occipital region, POC) and thalamic (centrodorsal part of reticular nucleus (RTN), dorsolateral thalamic nucleus (LD)) brain activity of juvenile piglets (n=8; mean ± SEM).

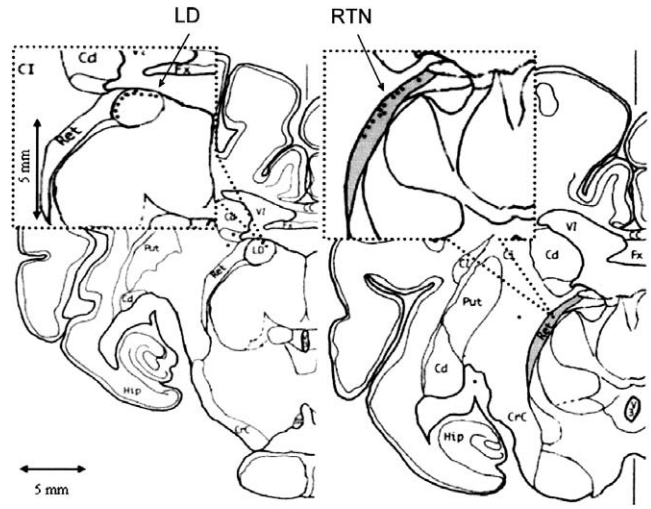

Fig. 6. Reticular (RTN, right panel) and dorsolateral (LD, left panel) thalamic nuclei (highlighted in grey) in frontal view (modified, according to Félix et al. 1999, with permission)[1] corresponding to the coordinates of electrodes location. The insets show the correctly placed electrodes. The corresponding false hits are presented in the large figures (Variation of correct electrode location in sagittal plane ± 1 mm). (Cc) Corpus callosum; (Cd) Nucl. caudatus; (CI) Capsula interna; (CrC) Crus cerebri superiorum; (Fx) Fornix; (Hip) Hippocampus; (LD) Nucl. lateralis dorsalis thalami; (Put) Putamen; (Ret) Nucl. reticularis thalami; (V3) Ventriculus tertius; (Vl) Ventriculus lateralis.

DISCUSSION

This contribution describes an easily practicable stereotactic approach for neurophysiological investigations of key thalamic structures of the juvenile domestic pig. Here, we used an electrophysiological characterization of different sedation procedures. A similar approach lends itself to study neurochemical monitoring using microdialysis or electrochemical sensors.

Placement of surface and deep electrodes and selection for electrophysiological analysis was performed owing to neurophysiology of reticulo-thalamocortical circuitry and technical considerations.

RTN is a non-specific reticular thalamic nucleus known for its central role in gating the afferent inputs from the periphery to the cortex (Steriade 2001). Despite absence of reports on pig, there are numerous data from rodents, rabbits and cats on somatotopic organization of RTN and its corticothalamic projections (Crabtree 1999, Deschenes et al. 1998, Ghazanfar and Nicolelis 2001, Jones 1985). The centrodorsal area of RTN chosen for electrode placement has been implied in gating the primary sensorymotor afferents to the cortex in rabbit, cat and monkey (Crabtree 1999, Jones 1985). This is also a stereotactically favorable location, since RTN is thicker in this area which makes it easier for targeting than its dorsal part.

LD was described in swine and is located directly below the lateral ventricle (Solnitzky 1938). This makes it easier for successful targeting *via* vertical electrode insertion. Robertson and coauthors (1980, 1983) have shown in cat and rat that LD receives afferent projections from several nuclei of the pretectal complex which, in turn, receives somatosensory afferents, and sends efferent projections to several subdivisions of limbic system. Thus, LD seems to represent a route whereby exteroceptive information could reach the limbic cortex and hippocampal formation (Jones 1985). Indeed, SEPs appeared in all three regions investigated after repeated trigeminal somatosensory stimulation.

A methodical advantage of targeting LD versus the specific sensorymotor thalamic nuclei of ventrobasal complex (Crabtree 1999) appears a sufficiently large distance between RTN and LD than between the chosen sector of RTN and aforementioned structures. Therefore, this approach provides a better model for electrophysiological study of reticulo-thalamocortical interactions using field potentials avoiding interfering effects of volume conduction on a distance less than 10 mm in the gyrencephalic brain (Bullock et al. 1995). These results suggest that somatosensory activity from trigeminal supply area is linked functionally with the centrodorsal area of RTN (Crabtree 1999).

The advantage of the herein presented stereotactic approach compared with previous procedures

[1] Reprinted from Brain Research Bulletin Vol. 49, issues 1–2, Félix B, Léger M-E, Albe-Fessard D, Marcilloux J-C, Rampin O, Laplace J-P, Duclos A, Fort F, Gougis S, Costa M, Duclos N, Stereotaxic atlas of the pig brain, p. 1–137. Copyright 1999, with permission from Elsevier.

(Marcilloux et al. 1989) is the use of a conventional and simple mode of implementation with satisfactory success rate. However, some degree of uncertainty in targeting always remains as our drop outs show. Another drawback is the fact that post mortem work up is necessary to prove localization due to some inevitable morphologic variation (as opposed to *in vivo* imaging, such as ventriculography (Marcilloux et al. 1989)).

Cardiovascular and brain metabolic data revealed anticipated alterations depending on drug effects. Blood pressure and heart rate as well as CBF and brain oxidative metabolism were reduced in general anesthesia induced by 1.3% isoflurane and 66% nitrous oxide in inspired gas, compared to the fentanyl induced analgesic stage. Administration of isoflurane and nitrous oxide result in concentrations used in this study corresponds to about 1.0 minimal alveolar concentration (MAC) abolishing the motor response to a standardized painful stimulus in one half of individuals studied (Shim and Andersen 1972). Previous studies reported 1.0 MAC during 2% isoflurane administration in juvenile pigs (Eger et al. 1988, Rampil et al. 1988). Additional administration of 66% nitrous oxide reduces the isoflurane MAC by 42% in swine (Eisele et al. 1985). The observed marked reduction of arterial blood pressure during isoflurane/nitrous oxide anesthesia reflects a pronounced reduction of total peripheral resistance (Eger 1981). However, myocardial function as well as cardiac output appear barely compromised under these conditions. In addition, redistribution of the circulating blood volume favors cerebral perfusion, whereas myocardial, hepatic and renal perfusion remains unaltered and splanchnic as well as skeletal blood flows decrease (Lundeen et al. 1983). Therefore, the observed reduction in CBF and brain oxidative metabolism is obviously caused by an appropriate depression of brain functional activity. We found a reduction in $CMRO_2$ and $CMR_{Glucose}$ by about one-fourth whereas CBF was reduced by one-fifth suggesting a mild cerebrovascular dilation effect of isoflurane (Eger 1981). In addition, it has been into consideration that a mild but significantly lower level of arterial pCO_2 was present during administration of isoflurane and nitrous oxide (Table I, $P<0.05$). Therefore we assume that the vasodilatory effect of isoflurane is obviously blunted by the reduced arterial pCO_2. The herein used fentanyl dosage warrants sufficient analgesia in young pigs (Rajan et al. 1998). Moreover, systemic cardiovascular effects of fentanyl analgesia are similar to those obtained from unsedated swine (Hannon et al. 1990).

Electrophysiological features of spontaneous and evoked brain activity revealed hints of some specific regional responses on the different modes of sedation and analgesia used. The results of ECoG spectral power analysis confirmed known findings associated with isoflurane and fentanyl sedations in pig (Pichlmayr et al. 1983). Synchronized low frequency band activity, typical of light to moderate sedation by volatile anesthetics, was markedly more pronounced in all regions studied, whereas a comparably elevated beta and gamma band activity was shown in RTN. This might be a result of RTN neurons being in burst firing mode under isoflurane sedation. In contrast, cortical and LD high frequency activity were similar in both states. However, in State 2 the spectral power decreased in LD in theta frequency band. This was paralleled by a change in coherence pattern with POC-LD coherence being now higher than POC-RTN coherence in high frequency bands. This is obviously an expression of a re-activation of LD's specific sensory relay function after having been inhibited by RTN in State 1. Underlying mechanisms cannot be verified in this setting. Previous studies suggest that activation of GABAergic inhibitory input as well as a decrease of the excitatory drive of thalamic glutamatergic relay neurons are responsible for the enhanced sedative effect of increasing isoflurane dosages in adult rats (Detsch et al. 2002). In rodents, GABAergic inhibitory input appears of major relevance for functional disconnection by volatile anesthetics, because local GABA(A) receptor blockade reverses isoflurane's suppressive effects on thalamic neurons (Caraiscos et al. 2004, Vahle-Hinz et al. 2001). Functional disconnection with impairment of thalamocortical transmission of sensory signals was also shown in humans suggesting block of thalamocortical information transfer as a key effect of sedation (Alkire et al. 2000, Antognini et al. 1997). Recent progress in directionality analysis seems to be a promising approach to characterize state-dependent coupling patterns in these neuronal networks (Winterhalder et al. 2005).

A relative proximity of the inserted RTN and LD electrodes (an average distance of 10 mm) makes it necessary to address the influence of volume conduction effect on our results. We found a complete loss of any RTN-LD coherence in gamma band of State 2. Consequently, the impact of volume conduction

between these recording sites with regard to activities in gamma band during both states was rather irrelevant. Furthermore, the RTN-LD coherence in State 1 was higher than POC-LD coherence in all frequency bands, whereas in State 2 no difference between them was found in beta band anymore. As the sedation became lighter in State 2, new functional properties seem to have become apparent in RTN-LD and POC-LD interactions in beta frequency band abolishing the likely predominant volume conduction effects in RTN-LD in State 1. Remarkably, RTN-LD coherence in State 1 was higher than POC-RTN coherence exclusively in delta frequency band. In contrast, in State 2 this is applied to all but gamma frequency bands. We assume that these results also reflect a functional change in reticulo-thalamocortical network activity induced by switch to fentanyl sedation thus favoring functional synaptic connectivity between these neuronal structures. These findings are supported by previous findings in different species where a dependence of coherence on frequency band and electrode distance has been reported (Bullock et al. 1995, Grieve et al. 2003, Nunez et al. 1999, Srinivasan et al. 1998).

CONCLUSION

An easy to implement approach was established, characterized and applied to study electrophysiological features of the reticulo-thalamocortical network in a juvenile pig model. Therefore, investigation of vigilance-dependent integrative brain functions can be performed.

ACKNOWLEDGMENTS

The authors thank Mrs. Ch. Ernst and Mr. L. Wunder for skilful technical assistance. The study was partly supported by Bundesministerium für Bildung und Forschung grant BMBF-FKZ 01 ZZ 0105 (R.B.).

REFERENCES

Alkire MT, Haier RJ, Fallon JH (2000) Toward a unified theory of narcosis: brain imaging evidence for a thalamocortical switch as the neurophysiologic basis of anesthetic-induced unconsciousness. Conscious Cogn 9: 370–386.

Andrews RJ, Knight RT, Kirby RP (1990) Evoked potential mapping of auditory and somatosensory cortices in the miniature swine. Neurosci Lett 114: 27–31.

Antognini JF, Buonocore MH, Disbrow EA, Carstens E (1997) Isoflurane anesthesia blunts cerebral responses to noxious and innocuous stimuli: A fMRI study. Life Sci 61: PL 349–354.

Bauer R, Walter B, Torossian A, Fritz H, Schlonski O, Jochum T, Hoyer D, Reinhart K, Zwiener U (1999) A piglet model for evaluation of cerebral blood flow and brain oxidative metabolism during gradual cerebral perfusion pressure decrease. Pediatr Neurosurg 30: 62–69.

Bauer R, Walter B, Wurker E, Kluge H, Zwiener U (1996) Colored microsphere technique as a new method for quantitative-multiple estimation of regional hepatic and portal blood flow. Exp Toxicol Pathol 48: 415–420.

Bullock TH, McClune MC, Achimowicz JZ, Iragui-Madoz VJ, Duckrow RB, Spencer SS (1995) Temporal fluctuations in coherence of brain waves. Proc Natl Acad Sci U S A 92: 11568–11572.

Caraiscos VB, Newell JG, You-Ten KE, Elliott EM, Rosahl TW, Wafford KA, MacDonald JF, Orser BA (2004) Selective enhancement of tonic GABAergic inhibition in murine hippocampal neurons by low concentrations of the volatile anesthetic isoflurane. J Neurosci 24: 8454–8458.

Coyle MG, Oh W, Stonestreet BS (1993) Effects of indomethacin on brain blood flow and cerebral metabolism in hypoxic newborn piglets. Am J Physiol 264: H141–149.

Crabtree JW (1999) Intrathalamic sensory connections mediated by the thalamic reticular nucleus. Cell Mol Life Sci 56: 683–700.

Dellmann H, McClure R (1966) Skull measurements for the establishment of a coordinate system for stereotaxic placement in the brain of swine (*Sus scrofa*). Swine in biomedical research. Proceedings of a Symposium at the Pacific Northwest Laboratories, Frayn Printing, Seattle, p. 537–542.

Deschenes M, Veinante P, Zhang ZW (1998) The organization of corticothalamic projections: Reciprocity versus parity. Brain Res Brain Res Rev 28: 286–308.

Detsch O, Kochs E, Siemers M, Bromm B, Vahle-Hinz C (2002) Differential effects of isoflurane on excitatory and inhibitory synaptic inputs to thalamic neurones in vivo. Br J Anaesth 89: 294–300.

Eger EI (1981) Isoflurane (Forane): A compendium and reference. Ohio Medical Products, Madison.

Eger EI, 2nd, Johnson BH, Weiskopf RB, Holmes MA, Yasuda N, Targ A, Rampil IJ (1988) Minimum alveolar concentration of I-653 and isoflurane in pigs: Definition of a supramaximal stimulus. Anesth Analg 67: 1174–1176.

Eisele PH, Talken L, Eisele JH, Jr. (1985) Potency of isoflurane and nitrous oxide in conventional swine. Lab Anim Sci 35: 76–78.

Félix B, Léger M-E, Albe-Fessard D, Marcilloux J-C, Rampin O, Laplace J-P, Duclos A, Fort F, Gougis S, Costa M, Duclos N (1999) Stereotaxic atlas of the pig brain. Brain Res Bull 49: 1–137.

Fiset P, Paus T, Daloze T, Plourde G, Meuret P, Bonhomme V, Hajj-Ali N, Backman SB, Evans AC (1999) Brain mechanisms of propofol-induced loss of consciousness in humans: a positron emission tomographic study. J Neurosci 19: 5506–5513.

Fritz H, Bauer R, Walter B, Schlonski O, Hoyer D, Zwiener U, Reinhart K (1999) Hypothermia related changes in electrocortical activity at stepwise increase of intracranial pressure in piglets. Exp Toxicol Pathol 51: 163–171.

Fritz HG, Walter B, Holzmayr M, Brodhun M, Patt S, Bauer R (2005) A pig model with secondary increase of intracranial pressure after severe traumatic brain injury and temporary blood loss. J Neurotrauma 22: 807–821.

Ghazanfar AA, Nicolelis MA (2001) Feature article: the structure and function of dynamic cortical and thalamic receptive fields. Cereb Cortex 11: 183–193.

Goel V, Brambrink AM, Baykal A, Koehler RC, Hanley DF, Thakor NV (1996) Dominant frequency analysis of EEG reveals brain's response during injury and recovery. IEEE Trans Biomed Eng 43: 1083–1092.

Grieve PG, Emerson RG, Fifer WP, Isler JR, Stark RI (2003) Spatial correlation of the infant and adult electroencephalogram. Clin Neurophysiol 114: 1594–1608.

Hannon JP, Bossone CA, Wade CE (1990) Normal physiological values for conscious pigs used in biomedical research. Lab Anim Sci 40: 293–298.

Jarvinen MK, Morrow-Tesch J, McGlone JJ, Powley TL (1998) Effects of diverse developmental environments on neuronal morphology in domestic pigs (Sus scrofa). Brain Res Dev Brain Res 107: 21–31.

Jones EG (1985) The Thalamus. Plenum Press, New York.

Kirsch JR, Helfaer MA, Blizzard K, Toung TJ, Traystman RJ (1990) Age-related cerebrovascular response to global ischemia in pigs. Am J Physiol 259: H1551–1558.

Kuhnen G, Bauer R, Walter B (1999) Controlled brain hypothermia by extracorporeal carotid blood cooling at normothermic trunk temperatures in pigs. J Neurosci Methods 89: 167–174.

Lundeen G, Manohar M, Parks C (1983) Systemic distribution of blood flow in swine while awake and during 1.0 and 1.5 MAC isoflurane anesthesia with or without 50% nitrous oxide. Anesth Analg 62: 499–512.

Marcilloux JC, Rampin O, Felix MB, Laplace JP, Albe-Fessard D (1989) A stereotaxic apparatus for the study of the central nervous structures in the pig. Brain Res Bull 22: 591–597.

Martoft L, Jensen EW, Rodriguez BE, Jorgensen PF, Forslid A, Pedersen HD (2001) Middle-latency auditory evoked potentials during induction of thiopentone anaesthesia in pigs. Lab Anim 35: 353–363.

Mount LE, Ingram DL (1971) The Pig as a laboratory animal. Academic Press, London.

Niedermeyer E, Da Silva FL (eds.) (1999) Electroencephalography: Basic Principles, Clinical Application and Related Field. Lippincott Williams & Wilkins, Baltimore.

Nunez PL, Silberstein RB, Shi Z, Carpenter MR, Srinivasan R, Tucker DM, Doran SM, Cadusch PJ, Wijesinghe RS (1999) EEG coherency II: experimental comparisons of multiple measures. Clin Neurophysiol 110: 469–486.

Okada Y, Lahteenmaki A, Xu C (1999) Comparison of MEG and EEG on the basis of somatic evoked responses elicited by stimulation of the snout in the juvenile swine. Clin Neurophysiol 110: 214–229.

Pace-Schott EF, Hobson JA (2002) The neurobiology of sleep: Genetics, cellular physiology and subcortical networks. Nat Rev Neurosci 3: 591–605.

Pichlmayr I, Lips U, Künkel H (1983) Electroencephalogram in Anesthesia. Fundamentals, Practical Application, Examples (in German). Springer-Verlag, Berlin.

Poceta JS, Hamlin MN, Haack DW, Bohr DF (1981) Stereotaxic placement of cannulae in cerebral ventricles of the pig. Anat Rec 200: 349–356.

Rajan V, Beharry KD, Williams P, Modanlou HD (1998) Pharmacodynamic effects and pharmacokinetic profile of continuous infusion fentanyl in newborn piglets. Biol Neonate 74: 39–47.

Rampil IJ, Weiskopf RB, Brown JG, Eger EI, 2nd, Johnson BH, Holmes MA, Donegan JH (1988) I653 and isoflurane produce similar dose-related changes in the electroencephalogram of pigs. Anesthesiology 69: 298–302.

Robertson RT, Kaitz SS, Robards MJ (1980) A subcortical pathway links sensory and limbic systems of the forebrain. Neurosci Lett 17: 161–165.

Robertson RT, Thompson SM, Kaitz SS (1983) Projections from the pretectal complex to the thalamic lateral dorsal nucleus of the cat. Exp Brain Res 51: 157–171.

Ross DT, Graham DI, Adams JH (1993) Selective loss of neurons from the thalamic reticular nucleus following severe human head injury. J Neurotrauma 10: 151–165.

Salinas-Zeballos ME, Zeballos GA, Gootman PM (1986) A stereotaxic atlas of the developing swine (Sus scrofa) forebrain. In: Swine in Biomedical Research (Tumbleson ME, ed.) Plenum Press, New York, p. 887–906.

Sherman DL, Brambrink AM, Ichord RN, Dasika VK, Koehler RC, Traystman RJ, Hanley DF, Thakor NV (1999) Quantitative EEG during early recovery from hypoxic-ischemic injury in immature piglets: Burst occurrence and duration. Clin Electroencephalogr 30: 175–183.

Shim CY, Andersen NB (1972) Minimal alveolar concentration (MAC) and dose-response curves in anesthesia. Anesthesiology 36: 146–151.

Solnitzky O (1938) The thalamic nuclei of Sus scrofa. J Comp Neurol 69: 121–169.

Srinivasan R, Nunez PL, Silberstein RB (1998) Spatial filtering and neocortical dynamics: Estimates of EEG coherence. IEEE Trans Biomed Eng 45: 814–826.

Steriade M (2001) The GABAergic reticular nucleus: A preferential target of corticothalamic projections. Proc Natl Acad Sci U S A 98: 3625–3627.

Vahle-Hinz C, Detsch O, Siemers M, Kochs E, Bromm B (2001) Local GABA(A) receptor blockade reverses isoflurane's suppressive effects on thalamic neurons in vivo. Anesth Analg 92: 1578–1584.

Walter B, Bauer R, Gaser E, Zwiener U (1997) Validation of the multiple colored microsphere technique for regional blood flow measurements in newborn piglets. Basic Res Cardiol 92: 191–200.

Walter B, Bauer R, Kuhnen G, Fritz H, Zwiener U (2000) Coupling of cerebral blood flow and oxygen metabolism in infant pigs during selective brain hypothermia. J Cereb Blood Flow Metab 20: 1215–1224.

Williams JC, Rennaker RL, Kipke DR (1999) Long-term neural recording characteristics of wire microelectrode arrays implanted in cerebral cortex. Brain Res Brain Res Protoc 4: 303–313.

Winterhalder M, Schelter B, Hesse W, Schwab K, Leistritz L, Klan D, Bauer R, Timmer J, Witte H (2005) Comparison of time series analysis techniques to detect direct and time-varying interrelations in multivariate, neural systems. Signal Process 85: 2137-2160.

Zwiener U, Schimke E, Prange H, Scholle S, Witte H, Glaser S, Schubert H, Zieger M (1983) Long-term recording of electrocortico- and electroencephalograms in the waking pig. I. Methods and methodological critique (in German). Z Versuchstierkd 25: 19–26.

Received 11 October 2005, accepted 9 March 2006